

# The frozen-field approximation and the Ginzburg–Landau equations of superconductivity

Hans G. Kaper<sup>1</sup> and Henrik Nordborg<sup>2</sup>

**Abstract.** The Ginzburg–Landau (GL) equations of superconductivity provide a computational model for the study of magnetic flux vortices in type-II superconductors. In this article we show through numerical examples and rigorous mathematical analysis that the GL model reduces to the frozen-field model when the charge of the Cooper pairs (the superconducting charge carriers) goes to zero while the applied field stays near the upper critical field.

**Key words:** Ginzburg–Landau equations, superconductivity, frozen-field approximation, asymptotic analysis.

## 1 Introduction

Superconducting materials hold great promise for technological applications. Especially since the discovery of the so-called high-temperature superconductors in the 1980s, much research has been devoted to understanding the behavior of these new materials. While conventional superconductors require liquid helium (3–4 degrees Kelvin) to remain in the superconducting state, high-temperature superconductors can be cooled with liquid nitrogen (76 degrees Kelvin)—a clear economic advantage. Unfortunately, high-temperature superconductors are ceramic materials, which are difficult to manufacture into films and wires, but progress is being made all the time.

High-temperature superconductors belong to the class of type-II superconductors. Unlike type-I superconductors, type-II superconductors can sustain a magnetic flux in their interior, but this flux is restricted to quantized amounts—filaments that are encircled by a current. The current shields the magnetic flux from the bulk, which is perfectly superconducting. The configuration resembles that of a vortex in a fluid, and the superconductor is said to be in the *vortex state*.

---

<sup>1</sup> Mathematics and Computer Science Division, Argonne National Laboratory, Argonne, IL 60439, USA ([kaper@mcs.anl.gov](mailto:kaper@mcs.anl.gov))

<sup>2</sup> James Franck Institute, The University of Chicago, 5640 South Ellis Avenue, Chicago, IL 60637, USA ([Henrik.Nordborg@anl.gov](mailto:Henrik.Nordborg@anl.gov))

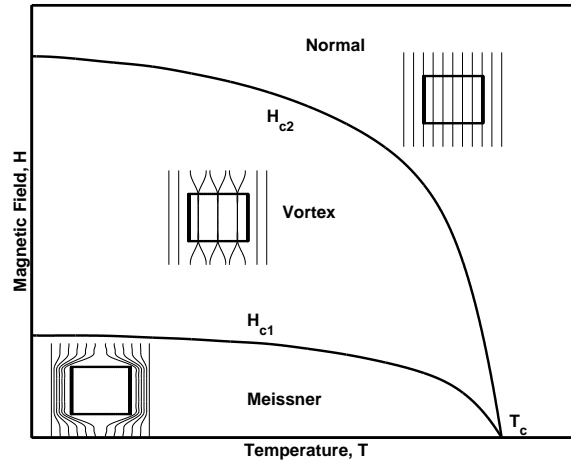


Figure 1: Phase diagram of a type-II superconductor.

Figure 1 gives a sketch of the phase diagram of a type-II superconductor in the neighborhood of  $T_c$ , the *critical temperature*. The two-dimensional phase space is spanned by the temperature  $T$  and the (magnitude of the) magnetic field  $H$  and is roughly divided into three subregions. Each subregion corresponds to a particular state: the perfectly superconducting (Meissner) state below the lower critical field  $H_{c1}$ , where no magnetic field can penetrate the medium; the normal state above the upper critical field  $H_{c2}$ , where the superconductor behaves like a normal metal; and the intermediate vortex state. Above the critical temperature  $T_c$  all superconducting properties are lost.

The vortices, and especially their dynamics, determine the current-carrying capabilities of a superconductor. Much effort, both experimental and theoretical, is therefore being spent on the study of vortex dynamics and, especially, mechanisms to inhibit vortex motion when the superconductor is subject to currents and fields. By “pinning” the vortices, one prevents energy dissipation and, hence, loss of superconductivity.

Vortices can be studied computationally at various levels of detail using different models. The Ginzburg–Landau (GL) model gives a field (continuum) description that, although phenomenological and not based on any microscopic quantum-mechanical theory, has been used successfully to study both the dynamics and the structure of vortex systems in realistic superconductor configurations [1, 2]. Figures 2 and 3 give two examples of computational results obtained with the GL equations. They illustrate both the effectiveness and the difficulties of such calculations.

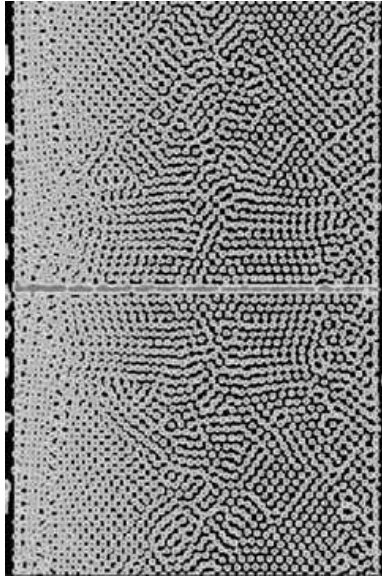


Figure 2: Vortex configuration in two dimensions.

Figure 2 shows a vortex configuration in a two-dimensional cross section of a twinned superconducting crystal, which was computed from a steady-state solution of the GL equations. The twin boundary (an irregularity in the structure of the crystal) is visible in the horizontal line through the center; it acts as a pinning site for the vortices. The field is perpendicular to the plane of the cross section, which measures  $128 \times 192$  coherence lengths (a characteristic length of the order of microns). Each dot corresponds to a vortex intersecting the plane of the cross section; the entire configuration has approximately 2,700 vortices. The figure shows the level of detail one can achieve with the GL model, given sufficient computing power. At the same time, it illustrates the level of computational complexity one faces if one uses the GL model.

Figure 3 shows a series of snapshots of a vortex configuration in three dimensions, also computed with the GL model. The objective of this computation was to simulate vortex motion through columnar defects and study the potential of the latter as pinning sites. The defects are visible as twisted straight lines. The vortices are the flexible tube-like structures; they move from one defect to another under the influence of external forces. The figure shows the motion of a vortex that is originally pinned on a defect. The vortex develops a loop, the loop peels off, the loop expands in both directions in a traveling-wave-like scenario, and gradually the entire vortex transfers to the next available defect.

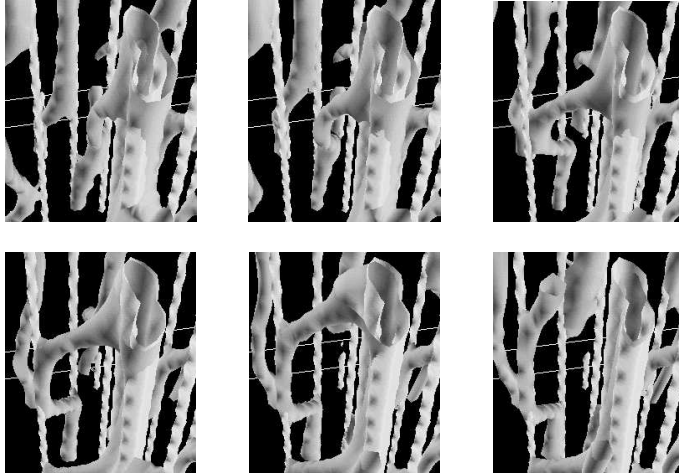


Figure 3: Kinking-induced motion of vortices through splayed columnar defects.

Numerical simulations provide the only way to study vortex dynamics at this level of detail. They are an invaluable tool for fundamental research, complementing experiment and theory. Numerical simulations of realistic superconductors based on the GL model, like the ones illustrated in Figs. 2 and 3 are, however, extremely time consuming, and it is desirable to use simpler models whenever possible. Here, we focus on the “frozen-field model,” which is still a continuum model and the closest approximation to the full GL model. In the frozen-field model, the superconducting phenomena are decoupled from the electromagnetic field, and the latter is prescribed through a vector potential. The frozen-field model is much simpler and has been used successfully for numerical simulations of vortex systems [3].

In this article, we prove that the frozen-field model is obtained as the asymptotic limit of the GL model when the charge of the Cooper pairs (the superconducting charge carriers) goes to zero while the applied magnetic field stays near the upper critical field. (The upper critical field itself depends on the charge of the Cooper pairs and increases as the latter decreases.) Because the temperature is constant in the GL model, this limit corresponds to fixing the temperature  $T$  and moving up vertically through the vortex regime to the curve labeled  $H_{c2}$  in the phase diagram of Fig. 1. The convergence rate is second order in the small parameter.

For more background on the physics of superconductivity we refer the reader to the monograph by Tinkham [4]. The original source for the GL equations of superconductivity is [5]. A good introduction to the mathematics of the GL equations is [6]. The dynamics of the GL equations have been studied by several authors;

see [7, 8, 9] and the references cited therein. The present investigation is closely related to the work of Du and Gray [10].

Section 2 introduces the Ginzburg–Landau equations, Section 3 contains the numerical results and Section 4 the analysis.

## 2 The Ginzburg–Landau equations

In the Ginzburg–Landau theory of superconductivity, the state of a superconducting medium is described by a complex scalar-valued *order parameter*  $\psi$  and a real vector-valued *vector potential*  $\mathbf{A}$ . If the state varies with time, a third variable—the *electric potential*  $\phi$ —is necessary to fully describe the electromagnetic field. The evolution of the state variables is governed by the time-dependent Ginzburg–Landau (TDGL) equations,

$$\gamma\hbar \left( \frac{\partial}{\partial t} + i\frac{q_s}{\hbar}\phi \right) \psi + \frac{1}{2m_s} \left( \frac{\hbar}{i}\nabla - \frac{q_s}{c}\mathbf{A} \right)^2 \psi + \alpha\psi + \beta|\psi|^2\psi = 0, \quad (2.1)$$

$$\sigma \left( -\frac{1}{c}\frac{\partial\mathbf{A}}{\partial t} - \nabla\phi \right) - \frac{c}{4\pi}\nabla \times \nabla \times \mathbf{A} + \mathbf{J}_s + \frac{c}{4\pi}\nabla \times \mathbf{H} = 0, \quad (2.2)$$

where the supercurrent density  $\mathbf{J}_s$  is a nonlinear function of  $\psi$  and  $\mathbf{A}$ ,

$$\mathbf{J}_s = \frac{q_s\hbar}{2im_s}(\psi^*\nabla\psi - \psi\nabla\psi^*) - \frac{q_s^2}{m_sc}|\psi|^2\mathbf{A} = \frac{q_s}{m_s}\Re \left[ \psi^* \left( \frac{\hbar}{i}\nabla - \frac{q_s}{c}\mathbf{A} \right) \psi \right]. \quad (2.3)$$

These equations are supplemented by the boundary conditions,

$$\mathbf{n} \cdot \mathbf{J}_s = 0, \quad \mathbf{n} \times (\nabla \times \mathbf{A}) = \mathbf{n} \times \mathbf{H}. \quad (2.4)$$

Here,  $\mathbf{H}$  is the *applied magnetic field*, which we assume to be time independent. The constants  $m_s$  and  $q_s$  are the mass and charge, respectively, of a Cooper pair (the superconducting charge carriers, also referred to as superelectrons);  $c$  is the speed of light; and  $\hbar$  is Planck’s constant divided by  $2\pi$ . A Cooper pair is made up of two electrons, each with charge  $-e$  ( $e$  is the elementary charge); hence,  $q_s$  is negative,  $q_s = -2e$ .

The parameters  $\alpha$  and  $\beta$  are material parameters;  $\alpha$  changes sign at the critical temperature  $T_c$ ,  $\alpha(T) < 0$  for  $T < T_c$  (superconducting state) and  $\alpha(T) > 0$  for  $T > T_c$  (normal state);  $\beta$  is only weakly temperature dependent and positive for all  $T$ .

The remaining parameters are  $\sigma$ , the normal state conductivity, and  $\gamma$ , the mobility coefficient. The latter is dimensionless and related to the diffusion coefficient  $D$ ,  $\gamma = \hbar/2m_s D$ .

The boundary conditions (2.4) express the fact that superelectrons cannot leave the superconductor. Also, if no surface currents are present, the tangential components of the magnetic field must be continuous across the boundary.

The parameters  $\alpha$  and  $\beta$  are defined phenomenologically, but they can be expressed in terms of measurable quantities, such as the superconducting *coherence length*  $\xi$  and the London *penetration depth*  $\lambda$ ,

$$\xi = \left( \frac{\hbar^2}{2m_s|\alpha|} \right)^{1/2}, \quad \lambda = \left( \frac{m_s c^2 \beta}{4\pi q_s^2 |\alpha|} \right)^{1/2}. \quad (2.5)$$

The coherence length and the London penetration depth define the respective characteristic length scales for the order parameter and the magnetic induction. Both depend on the temperature  $T$  and diverge as  $T$  approaches the critical temperature  $T_c$ , because of the factor  $|\alpha|^{-1/2}$ . However, their ratio is, to a good approximation, independent of temperature. This ratio is the *Ginzburg-Landau parameter*,

$$\kappa = \lambda/\xi. \quad (2.6)$$

In high- $T_c$  superconductors,  $\kappa$  is of the order of 50–100.

The electromagnetic variables are the *magnetic induction*  $\mathbf{B}$ , the *current density*  $\mathbf{J}$ , and the *electric field*  $\mathbf{E}$ ; they are given in terms of  $\mathbf{A}$  and  $\phi$  by the expressions

$$\mathbf{B} = \nabla \times \mathbf{A}, \quad \mathbf{J} = \frac{c}{4\pi} \nabla \times \nabla \times \mathbf{A}, \quad \mathbf{E} = -\frac{1}{c} \frac{\partial \mathbf{A}}{\partial t} - \nabla \phi. \quad (2.7)$$

Equation (2.2) is essentially Ampère’s law,  $\mathbf{J} = (c/4\pi)\nabla \times \mathbf{B}$ , where the current  $\mathbf{J}$  is the sum of the supercurrent  $\mathbf{J}_s$ , the transport current  $\mathbf{J}_t = (c/4\pi)\nabla \times \mathbf{H}$ , and a “normal” current  $\mathbf{J}_n = \sigma \mathbf{E}$  (Ohm’s law). Hence, the GL model uses a quasistatic version of Maxwell’s equations, where the time derivative of the electric field is ignored.

The TDGL equations were first given by Schmid [11] in 1966 and subsequently derived from the microscopic theory of superconductivity by Gor’kov and Eliashberg [12]. Our notation is the same as in Gor’kov and Kopnin [13].

The solution of the TDGL equations is not unique. Any solution  $(\psi, \mathbf{A}, \phi)$  defines a family of solutions  $G_\chi(\psi, \mathbf{A}, \phi)$  parameterized by a sufficiently smooth function  $\chi$  of space and time,

$$G_\chi : (\psi, \mathbf{A}, \phi) \mapsto \left( \psi e^{i(q_s/\hbar c)\chi}, \mathbf{A} + \nabla \chi, \phi - \frac{1}{c} \frac{\partial \chi}{\partial t} \right). \quad (2.8)$$

This property is known as *gauge invariance*; the function  $\chi$  is known as a *gauge function*. Gauge invariance does not affect the physically measurable quantities (the magnetic induction  $\mathbf{B}$ , the magnetization  $\mathbf{M} = \mathbf{B} - \mathbf{H}$ , and the current density  $\mathbf{J}$ ). Uniqueness requires an additional constraint, which is imposed through a gauge choice. The choice of a proper gauge for the TDGL equations has been a subject of considerable debate. The choice is a matter of convenience and may depend on the problem under investigation. In this article we adopt a gauge in which, at any time, the electric potential and the divergence of the vector potential satisfy the identity

$$\sigma\phi + (c/4\pi)\nabla \cdot \mathbf{A} = 0 \quad (2.9)$$

everywhere in the domain, while  $\mathbf{A}$  is tangential at the boundary. This choice is realized by identifying the gauge  $\chi$  with a solution of the linear parabolic equation

$$\frac{\sigma}{c} \frac{\partial \chi}{\partial t} - \frac{c}{4\pi} \Delta \chi = \sigma\phi + \frac{c}{4\pi} \nabla \cdot \mathbf{A}, \quad (2.10)$$

subject to the condition  $\mathbf{n} \cdot \nabla \chi = -\mathbf{n} \cdot \mathbf{A}$  on the boundary. In [9], it was shown that the TDGL equations, subject to the constraint (2.9), define a dynamical system under suitable regularity conditions on  $\mathbf{H}$ . (In the more general case, where  $\mathbf{H}$  varies not only in space but also in time, the TDGL equations define a dynamical process.) This dynamical system has a global attractor, which consists of the stationary points of the dynamical system and the heteroclinic orbits connecting such stationary points. Furthermore, it was shown that every solution on the attractor satisfies the condition  $\nabla \cdot \mathbf{A} = 0$  (and, therefore, also  $\phi = 0$ ). Thus, in the limit as  $t \rightarrow \infty$ , every solution of the TDGL equations satisfies the GL equations in the London gauge.

## 2.1 Nondimensional TDGL equations

In this section, we render the TDGL equations dimensionless by choosing units for the independent and dependent variables. Since we are interested in the collective behavior of vortices in the bulk of a superconductor in the limit of weak coupling ( $q_s \rightarrow 0$ ), we take care to choose the units in such a way that they remain of order one as  $q_s \rightarrow 0$ . (We recall that  $q_s$  is negative,  $q_s = -2e$ .)

As  $q_s \rightarrow 0$ , the coherence length  $\xi$  remains of order one, while the penetration depth  $\lambda$  increases like  $|q_s|^{-1}$ ; see Eq. (2.5). This suggests taking the coherence length  $\xi$  as the unit of length.

To maintain the diffusion coefficient  $D = \hbar/2\gamma m_s = \xi^2(\gamma\hbar/|\alpha|)^{-1}$  at order one, we measure time in units of  $\gamma\hbar/|\alpha|$ .

The real and imaginary parts of the order parameter are conveniently measured in units of  $\psi_0 = (|\alpha|/\beta)^{1/2}$ , which is the value of  $\psi$  that minimizes the free energy in the absence of a field.

Next, consider the magnetic field. A fundamental quantity in the theory of type-II superconductors is the flux quantum  $\Phi_0$ ,

$$\Phi_0 = \frac{hc}{|q_s|} = 2\pi \frac{\hbar c}{|q_s|}. \quad (2.11)$$

The flux quantum is the unit of magnetic flux carried by a vortex. Together with the coherence length and penetration depth, it defines three characteristic field strengths: the *lower critical field*  $H_{c1}$ , the *thermodynamical critical field*  $H_c$ , and the *upper critical field*  $H_{c2}$ ,

$$H_{c1} = \frac{\Phi_0}{4\pi\lambda^2 \ln \kappa}, \quad H_c = \frac{\Phi_0}{2\pi\xi\lambda\sqrt{2}}, \quad H_{c2} = \frac{\Phi_0}{2\pi\xi^2}. \quad (2.12)$$

Below  $H_{c1}$ , a superconductor is in the ideal superconducting (Meissner) state, where it does not support magnetic flux in the bulk; above  $H_{c2}$ , it is in the normal state, where the magnetic flux is distributed uniformly in the bulk; between  $H_{c1}$  and  $H_{c2}$ , it is in the vortex state, where magnetic flux is quantized in vortex-like configurations (see Fig. 1). The thermodynamical critical field  $H_c$  is intermediate between  $H_{c1}$  and  $H_{c2}$  and is defined by the identity  $H_c^2/8\pi = \frac{1}{2}\psi_0^2|\alpha|$ ;  $H^2/8\pi$  is the energy per unit volume associated with a field  $H$ , and  $\frac{1}{2}\psi_0^2|\alpha|$  is the minimum condensation energy, which is attained when  $\psi = \psi_0$ , so these two quantities are in balance when  $H = H_c$ .

As  $q_s \rightarrow 0$ ,  $H_{c1}$  goes to 0 like  $|q_s|$ ,  $H_c$  remains of order one, and  $H_{c2}$  grows like  $|q_s|^{-1}$ . This suggests that we define field strengths in terms of  $H_c$ . In fact, it is convenient to absorb a factor  $\sqrt{2}$ , so we adopt  $H_c\sqrt{2}$  or, equivalently,  $\hbar c/\xi\lambda|q_s|$  as the unit for the magnetic field strength.

With the coherence length as the unit of length and  $H_c\sqrt{2}$  as the unit of field strength, it follows that the vector potential is measured in units of  $\xi H_c\sqrt{2}$ . Furthermore, energy densities are measured in units of  $H_c^2/4\pi$ , which is the same as  $|\alpha|\psi_0^2$ .

Finally, we define the scalar potential  $\phi$  in units of  $(1/\gamma\psi_0^2\kappa|q_s|)(H_c^2/4\pi)$ . Notice that this unit remains of order one as  $q_s \rightarrow 0$ , because  $\kappa|q_s|$  is of order one. On the other hand, the product  $q_s\phi$ , which represents an energy density, tends to zero as  $q_s \rightarrow 0$ . (It remains finite on the scale of the penetration depth.)

Table 1 summarizes the relations between the original variables and their non-dimensional (primed) counterparts. We adopt the latter as the new variables and work



until further notice on the nondimensional problem. We omit all primes.

Table 1: Nondimensionalization.

Independent variables	$\mathbf{x} = \xi \mathbf{x}'$ $t = (\gamma \hbar /  \alpha ) t'$
Dependent variables	$\psi = \psi_0 \psi'$ $\mathbf{A} = (\xi H_c \sqrt{2}) \mathbf{A}'$ $\phi = (1 / \gamma \psi_0^2 \kappa  q_s ) (H_c^2 / 4\pi) \phi'$
Electromagnetic variables	$\mathbf{B} = (H_c \sqrt{2}) \mathbf{B}'$ $\mathbf{J} = (c H_c \sqrt{2} / 4\pi \xi) \mathbf{J}'$ $\mathbf{E} = (1 / \gamma \psi_0^2 \kappa  q_s ) (H_c^2 / 4\pi \xi) \mathbf{E}'$
Applied field	$\mathbf{H} = (H_c \sqrt{2}) \mathbf{H}'$
Normal conductivity	$\sigma = (\gamma m_s c^2 / 2\pi \hbar) \sigma'$

The nondimensional TDGL equations are

$$\left( \frac{\partial}{\partial t} - \frac{i}{\kappa} \phi \right) \psi - \left( \nabla + \frac{i}{\kappa} \mathbf{A} \right)^2 \psi - (1 - |\psi|^2) \psi = 0, \quad (2.13)$$

$$\sigma \frac{\partial \mathbf{A}}{\partial t} - \Delta \mathbf{A} - \frac{1}{\kappa} \mathbf{J}_s - \nabla \times \mathbf{H} = \mathbf{0}, \quad (2.14)$$

where

$$\mathbf{J}_s = -\frac{1}{2i} (\psi^* \nabla \psi - \psi \nabla \psi^*) - \frac{1}{\kappa} |\psi|^2 \mathbf{A} = -\Im \left[ \psi^* \left( \nabla + \frac{i}{\kappa} \mathbf{A} \right) \psi \right], \quad (2.15)$$

with the corresponding gauge condition,

$$\sigma \phi + \nabla \cdot \mathbf{A} = 0. \quad (2.16)$$

In deriving Eq. (2.14), we have made use of the gauge condition (2.16) and the vector identity

$$\Delta \mathbf{A} = -\nabla \times \nabla \times \mathbf{A} + \nabla (\nabla \cdot \mathbf{A}). \quad (2.17)$$

If  $\Omega$  is the domain occupied by the superconducting material (measured in units of  $\xi$ ), then Eqs. (2.13)–(2.16) must be satisfied everywhere  $\Omega$ . At the boundary  $\partial\Omega$  of  $\Omega$ , we have the conditions

$$\mathbf{n} \cdot \mathbf{J}_s = 0, \quad \mathbf{n} \times (\nabla \times \mathbf{A}) = \mathbf{n} \times \mathbf{H}, \quad \mathbf{n} \cdot \mathbf{A} = 0. \quad (2.18)$$

Here,  $\mathbf{n}$  is the local unit normal vector.

The electromagnetic variables are given by the expressions

$$\mathbf{B} = \nabla \times \mathbf{A}, \quad \mathbf{J} = \nabla \times \nabla \times \mathbf{A}, \quad \mathbf{E} = -\partial_t \mathbf{A} - \nabla \phi. \quad (2.19)$$

The values of the lower and upper critical fields are

$$H_{c1} = (2\kappa \ln \kappa)^{-1}, \quad H_{c2} = \kappa. \quad (2.20)$$

## 2.2 Link variables

The combination  $\nabla + (i/\kappa)\mathbf{A}$  plays a fundamental role; we refer to it as the  $\mathbf{A}$ -gradient and write

$$\nabla_{\mathbf{A}} = \nabla + \frac{i}{\kappa}\mathbf{A}. \quad (2.21)$$

The  $\mathbf{A}$ -gradient defines the  $\mathbf{A}$ -Laplacian (or “twisted Laplacian”),

$$\Delta_{\mathbf{A}} = \nabla_{\mathbf{A}} \cdot \nabla_{\mathbf{A}} = \left( \nabla + \frac{i}{\kappa}\mathbf{A} \right)^2. \quad (2.22)$$

The relation between the  $\mathbf{A}$ -Laplacian and the ordinary Laplacian is most easily illustrated by means of the *link variables*,

$$\begin{aligned} U_x(x, y, z) &= \exp\left(\frac{i}{\kappa} \int^x A_x(\xi, y, z) d\xi\right), \\ U_y(x, y, z) &= \exp\left(\frac{i}{\kappa} \int^y A_y(x, \eta, z) d\eta\right), \\ U_z(x, y, z) &= \exp\left(\frac{i}{\kappa} \int^z A_z(x, y, \zeta) d\zeta\right). \end{aligned} \quad (2.23)$$

(We omit the argument  $t$ .) The integrals are evaluated with respect to an arbitrary reference point. Each  $U_\mu$  ( $\mu = x, y, z$ ) is complex valued and unimodular,  $U_\mu^* = U_\mu^{-1}$ . The vectors  $\mathbf{A}$  and  $\mathbf{U}$  may be used interchangeably. With a slight abuse of notation, we have

$$\mathbf{U} = e^{(i/\kappa) \int \mathbf{A}}, \quad \nabla_{\mathbf{A}} = U^* \nabla U, \quad \Delta_{\mathbf{A}} = U^* \Delta U. \quad (2.24)$$

## 3 Numerical solution

A parallel code for solving Eqs. (2.13)–(2.18) has been developed as part of a project for large-scale simulations of vortex dynamics in superconductors. Details on these

simulations and on the code will be published elsewhere; here, we give only a brief overview of the numerical methods and the results of numerical simulations showing the behavior of the solution as  $\kappa$  increases.

The algorithm uses finite differences on a staggered grid, making all approximations accurate to second order in the mesh widths, and an implicit method for the time integration, making the algorithm (essentially) unconditionally stable. The code, written in C++, has been designed for a multiprocessing environment; it uses MPI for message passing.

We restrict the discussion to rectangular two-dimensional configurations that are periodic in one direction and open in the other. The configurations are assumed to be infinite in the third, orthogonal direction, which is also the direction of the applied magnetic field,  $\mathbf{H} = (0, 0, H_z)$ .

### 3.1 Discretization

**Computational grid.** The computational grid is uniform, with equal mesh sizes in the  $x$  and  $y$  direction,  $h_x = h_y = h$ . A vertex on the grid is denoted by  $\mathbf{x}_{i,j} = (x_i, y_j)$  and is the point of reference for the grid cell shown in Fig. 4. The indices run through

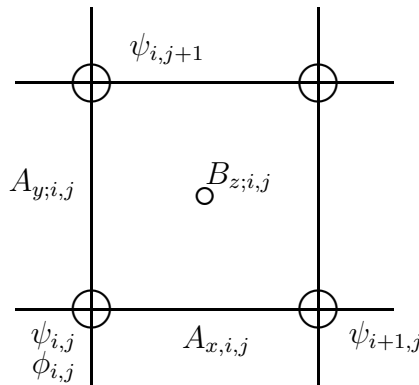


Figure 4: Computational grid cell and definition of the discrete variables.

the values  $i = 1, \dots, N_x$  and  $j = 1, \dots, N_y$ . We assume periodicity in the  $x$  direction and take the grid so the vertices with  $j = 1$  and  $j = N_y$  are located on the open boundary of the superconductor. Thus, the size of the domain is  $S = N_x(N_y - 1)h^2$ .

**Variables.** The discrete variables are introduced so that all derivatives are given by second-order accurate central-difference approximations. The scalar variables  $\psi$  and  $\phi$  are defined on the vertices of the grid,

$$\psi_{i,j} = \psi(\mathbf{x}_{i,j}), \quad \phi_{i,j} = \phi(\mathbf{x}_{i,j}). \quad (3.1)$$

(We use the same symbol for the original field and its discrete counterpart.) Vectors are defined at the midpoints of the links connecting adjacent vertices,

$$A_{x;i,j} = A_x(\mathbf{x}_{i,j} + \frac{1}{2}h_x\mathbf{e}_x), \quad A_{y;i,j} = A_y(\mathbf{x}_{i,j} + \frac{1}{2}h_y\mathbf{e}_y). \quad (3.2)$$

Here,  $\mathbf{e}_x$  and  $\mathbf{e}_y$  denote the unit vectors in the  $x$  and  $y$  direction, respectively. The definition of the discrete supercurrent  $\mathbf{J}_s$  is completely analogous. The link variables, defined in Eq. (2.24), are obtained from the vector potential,

$$U_{x;i,j} = e^{(i/\kappa)A_{x;i,j}h_x}, \quad U_{y;i,j} = e^{(i/\kappa)A_{y;i,j}h_y}. \quad (3.3)$$

They are therefore also defined on the links. Finally, the magnetic induction  $\mathbf{B}$ , which is a vector perpendicular to the plane and given by the curl of the vector potential, is defined at the center of a grid cell,

$$B_{z;i,j} = B_z(\mathbf{x}_{i,j} + \frac{1}{2}h_x\mathbf{e}_x + \frac{1}{2}h_y\mathbf{e}_y). \quad (3.4)$$

The definition of the discrete variables is also illustrated in Fig. 4.

Note that, because of the location of the grid relative to the boundaries, all scalar variables, as well as the  $x$  components of all vectors ( $A_x$ ,  $U_x$ ,  $J_{s,x}$ , and so forth), are defined on a  $N_x \times N_y$  grid, whereas the  $y$  components of all vectors and the magnetic induction  $B_z$  are defined on a  $N_x \times (N_y - 1)$  grid.

**Boundary conditions.** We assume periodicity in the  $x$  direction, so we need to consider the boundary conditions (4.7) only at  $y = y_1$  and  $y = y_{N_y}$ .

The boundary condition for the order parameter,  $\mathbf{n} \cdot \nabla_{\mathbf{A}}\psi = 0$ , becomes

$$U_{y;i,1}\psi_{i,2} - \psi_{i,1} = 0, \quad \psi_{i,N_y} - U_{y;i,N_y-1}^*\psi_{i,N_y-1} = 0, \quad (3.5)$$

for  $i = 1, \dots, N_x$ . For the vector potential, we require that  $\partial_y A_x = H_z$  and  $A_y$  is constant ( $A_y = 0$ ) on the boundary.

**Operators.** The gradient of a scalar is a vector and is therefore defined at the midpoint of a link connecting two adjacent vertices. Thus,

$$(\nabla\phi)_{x;i,j} = (\partial_x\phi)(\mathbf{x}_{i,j} + \frac{1}{2}h_x\mathbf{e}_x) = h_x^{-1}(\phi_{i+1,j} - \phi_{i,j}), \quad (3.6)$$

with an analogous definition for the  $y$  component. The gauge-invariant  $\mathbf{A}$ -gradient  $\nabla_{\mathbf{A}} = \nabla + i\mathbf{A}$  is defined in a similar way, with

$$(\nabla_{\mathbf{A}}\psi)_{x;i,j} = h_x^{-1}(\psi_{i+1,j}U_{x;i,j} - \psi_{i,j}). \quad (3.7)$$

Thus, the discrete version of the twisted Laplacian  $\Delta_{\mathbf{A}}$  is

$$\begin{aligned} (\Delta_{\mathbf{A}}\psi)_{i,j} &= h_x^{-2}(\psi_{i+1,j}U_{x;i,j} - 2\psi_{i,j} + \psi_{i-1,j}U_{x;i-1,j}^*) \\ &\quad + h_y^{-2}(\psi_{i,j+1}U_{y;i,j} - 2\psi_{i,j} + \psi_{i,j-1}U_{x;i,j-1}^*). \end{aligned} \quad (3.8)$$

The discrete version of the (normal) Laplacian is defined in the usual way,

$$(\Delta\psi)_{i,j} = h_x^{-2}(\psi_{i+1,j} - 2\psi_{i,j} + \psi_{i-1,j}) + h_y^{-2}(\psi_{i,j+1} - 2\psi_{i,j} + \psi_{i,j-1}). \quad (3.9)$$

The magnetic induction, which is the curl of the vector potential, takes the form

$$B_{z;i,j} = h_x^{-1}(A_{y;i+1,j} - A_{y;i,j}) - h_y^{-1}(A_{x;i,j+1} - A_{x;i,j}). \quad (3.10)$$

We also need the divergence of the vector potential, which is given by

$$(\nabla \cdot \mathbf{A})_{i,j} = h_x^{-1}(A_{x;i,j} - A_{x;i-1,j}) + h_y^{-1}(A_{y;i,j} - A_{y;i,j-1}). \quad (3.11)$$

**Algorithm.** For numerical purposes, it is useful to treat the TDGL equations (4.3) and (4.4) as two separate equations, which are coupled only through certain fields and variables. The electromagnetic potentials  $\phi$  and  $\mathbf{A}$  are treated as static variables in the order parameter equation,

$$(\partial_t - (i/\kappa)\phi)\psi - \Delta_{\mathbf{A}}\psi - (1 - |\psi|^2)\psi = 0. \quad (3.12)$$

The local nonlinear part of this equation,

$$(\partial_t - (i/\kappa)\phi)\psi - (1 - |\psi|^2)\psi = 0, \quad (3.13)$$

is integrated in the simplest possible manner,

$$\psi_{i,j}(t + \Delta t) = e^{-(i/\kappa)\phi_{i,j}\Delta t} \left\{ \psi_{i,j}(t) + \Delta t \left( 1 - |\psi_{i,j}|^2 \right) \psi_{i,j} \right\}. \quad (3.14)$$

The nonlocal part,

$$\partial_t \psi - \Delta_{\mathbf{A}} \psi = 0, \quad (3.15)$$

is integrated by using a backward Euler method, where the linear equation system is solved with the conjugate gradient method.

The equation for the vector potential,

$$\sigma \partial_t \mathbf{A} - \Delta \mathbf{A} - (1/\kappa) \mathbf{J}_s - \nabla \times \mathbf{H} = \mathbf{0}, \quad (3.16)$$

is linear and depends only indirectly on the order parameter through the supercurrent. If we treat the supercurrent as a static variable, we can integrate the equation easily, again using the backward Euler method. In the actual implementation, we use the fact that the domain is periodic to do a fast Fourier transform in the  $x$  direction, which leaves us with a tridiagonal system to solve in the  $y$  direction. This procedure is considerably faster than using an iterative method, such as the conjugate gradient method.

## 3.2 Numerical results

We use a rectangular sample, periodic in the  $x$  direction and open in the  $y$  direction, with  $N_x = N_y = 128$ . We take  $h_x = h_y = \frac{1}{2}\xi$ , so the sample measures 64 coherence lengths in the periodic direction and 63.5 coherence lengths across. (The coherence length  $\xi$  is defined in Eq. (2.5).)

First, we considered this system with  $\kappa = 200$  and an applied magnetic field  $H_z = 0.088\kappa$ . With a relatively large value of  $\kappa$ , the surface barrier for vortex entry is low, and the system equilibrates relatively fast [14, 15]. The equilibration required  $5 \times 10^4$  time steps with  $\Delta t = 0.4$ . The magnetic field produces an almost perfect vortex lattice. Figure 5 gives a contour plot of the density of Cooper pairs  $|\psi|^2$  at equilibrium; the zeros correspond to the centers of the vortices.

We then started from the configuration of Fig. 5 to find equilibrium configurations for other values of  $\kappa$ , varying  $\kappa$  from  $\kappa_{\min} = 40$  to  $\kappa_{\max} = 800$ . In this range, the ground states are comparable and similar to the one shown in Fig. 5. Since the magnetization of a sample is proportional to  $1/\kappa^2$ , the vortex density decreases with  $\kappa$ ; below  $\kappa_{\min}$ , the equilibrium state has fewer vortices, and a comparison becomes meaningless. Each equilibration required another  $3 \times 10^4$  time steps.

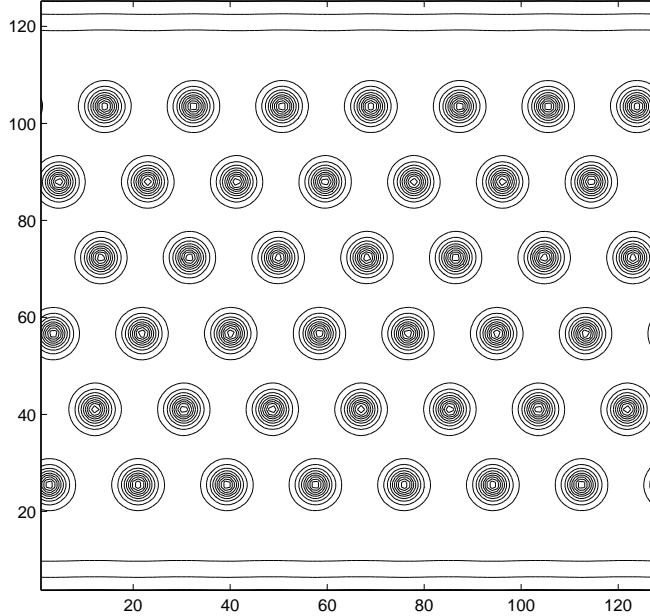


Figure 5: Contours of the density of Cooper pairs,  $|\psi|^2$ , for a system with  $\kappa = 200$ .

Figure 6 gives the computed values of the quantities

$$\delta\psi = \|\psi_\kappa - \psi_{\kappa_{\max}}\|_{L^2}, \quad \delta B_z = \frac{\|B_{z,\kappa} - B_{z,\kappa_{\max}}\|_{L^2}}{\|H_z\|_{L^2}}, \quad (3.17)$$

for different values of  $\kappa$ . The data show a behavior like  $1/\kappa^2$  down to  $\kappa \approx 40$ .

Figure 7 shows the average over  $x$  of  $A_{x,\kappa} - A_{x,\kappa_{\max}}$  as a function of  $y$  in the bulk of the sample, for different values of  $\kappa$ .

The numerical results show that the solution of the TDGL equations converges as  $\kappa$  increases; in fact, they show quadratic convergence in the small parameter  $1/\kappa$ . Given the fact that the Ginzburg–Landau parameter of high- $T_c$  superconducting materials is of the order of 50–100, we conclude that the limiting equation is a practical alternative in many applications. The question thus becomes: What is the limiting equation, and can we confirm the numerical conclusions by rigorous arguments? We address this question in the next section.

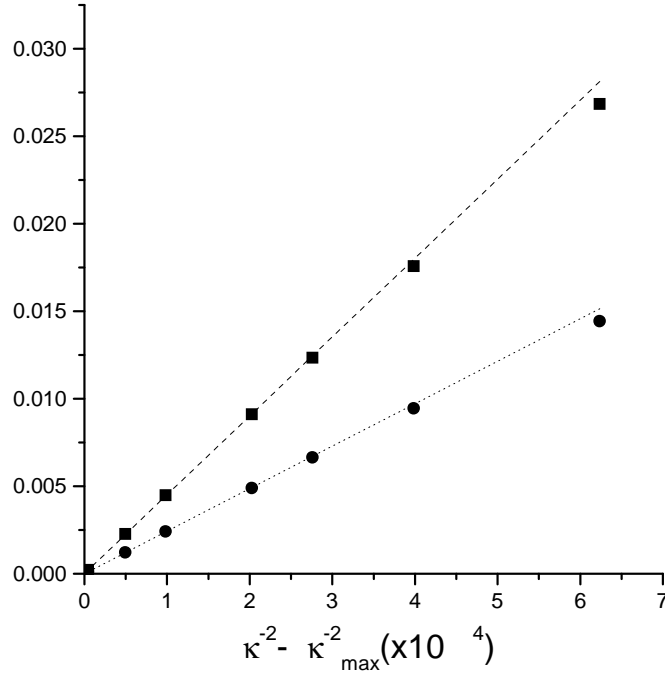


Figure 6: The quantities  $\delta\psi$  (solid squares) and  $\delta B_z$  (solid discs) for  $\kappa = 40, 50, 60, 70, 100, 140, 400, 800$ . The straight lines correspond to  $1/\kappa^2$  behavior.

## 4 Asymptotic analysis

We now return to the TDGL equations (2.13)–(2.18) and consider their limit as  $\kappa \rightarrow \infty$ . These are our standing hypotheses:

- (H1)  $\Omega$  is bounded in  $\mathbf{R}^n$  ( $n = 2, 3$ ), with a sufficiently smooth boundary  $\partial\Omega$ , for example,  $\partial\Omega$  of class  $C^{1,1}$ .
- (H2) The parameters  $\kappa$  and  $\sigma$  are real and positive.
- (H3)  $\mathbf{H}$  is independent of time; as a function of position, it satisfies the regularity condition  $\mathbf{H} \in [W^{\alpha,2}(\Omega)]^n$  for some  $\alpha \in (\frac{1}{2}, 1)$ .
- (H4)  $\kappa \gg 1$ ;  $\sigma = O(1)$  and  $\mathbf{H} = O(\kappa)$  as  $\kappa \rightarrow \infty$ .



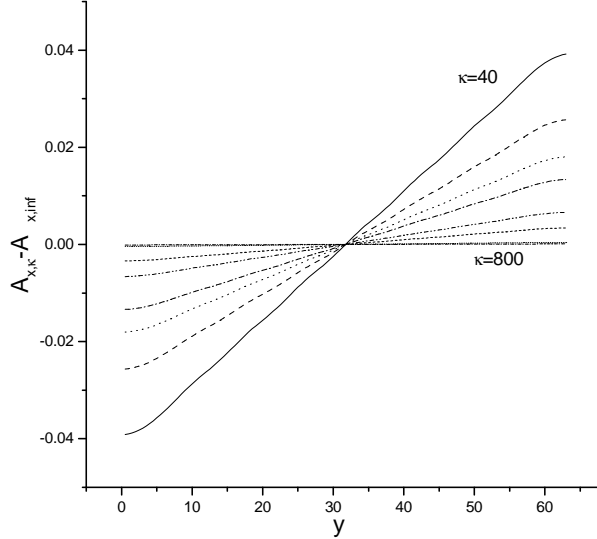


Figure 7: The average  $\langle A_{x,\kappa} - A_{x,\kappa_{\max}} \rangle$  vs.  $y$  for  $\kappa = 40, 50, 60, 70, 100, 140, 400, 800$ .

The assumptions **(H1)**–**(H3)** suffice to prove that the TDGL equations define a dynamical system in the Hilbert space

$$\mathcal{W}^{1+\alpha,2} = [W^{1+\alpha,2}(\Omega)]^2 \times [W^{1+\alpha,2}(\Omega)]^n; \quad (4.1)$$

see [9]. The space  $W^{1+\alpha,2}(\Omega)$  is continuously imbedded in  $W^{1,2}(\Omega) \cap L^\infty(\Omega)$ , so  $\psi$  and  $\mathbf{A}$  are bounded and differentiable with square-integrable (generalized) derivatives. **(H4)** is the operative hypothesis for the asymptotic analysis.

## 4.1 Mathematical analysis

**Scaling.** We begin by scaling the TDGL equations, taking into account the fact that we are interested in the limit as  $q_s \rightarrow 0$  (*weak coupling*), when the applied field is near the upper critical field. The scaling is done by means of the dimensionless GL parameter  $\kappa$ , which grows like  $|q_s|^{-1}$ .

Since  $\mathbf{H} = O(\kappa)$  as  $\kappa \rightarrow \infty$ , we begin by scaling  $\mathbf{H}$  by a factor  $\kappa$ ,  $\mathbf{H} = \kappa \mathbf{H}'$ . By scaling the vector potential by the same factor  $\kappa$ , we achieve that the electromagnetic variables are all of the same order.

The scalar potential is proportional to the charge density of the Cooper pairs, which is  $O(|q_s|)$  as  $q_s \rightarrow 0$ . Hence,  $\kappa\phi$  remains of order one. This suggests scaling  $\phi$  by a factor  $\kappa^{-1}$ .

Table 2 summarizes the relation between the current (nondimensional) variables and their scaled (primed) counterparts. We adopt the latter as the new variables and work until further notice on the scaled problem. We omit all primes.

Table 2: Scaling.

Applied Field	$\mathbf{H} = \kappa\mathbf{H}'$
Dependent variables	$\psi = \psi'$
	$\mathbf{A} = \kappa\mathbf{A}'$ $\phi = \kappa^{-1}\phi'$
Electromagnetic variables	$\mathbf{B} = \kappa\mathbf{B}'$
	$\mathbf{J} = \kappa\mathbf{J}'$ $\mathbf{E} = \kappa\mathbf{E}'$

After scaling, the relevant parameter is  $\kappa^2$ , rather than  $\kappa$ , so we introduce  $\varepsilon$ ,

$$\varepsilon = \kappa^{-2}. \quad (4.2)$$

The scaled TDGL equations are

$$(\partial_t - i\varepsilon\phi)\psi - (\nabla + i\mathbf{A})^2\psi - (1 - |\psi|^2)\psi = 0, \quad (4.3)$$

$$\sigma\partial_t\mathbf{A} - \Delta\mathbf{A} - \varepsilon\mathbf{J}_s - \nabla \times \mathbf{H} = \mathbf{0}, \quad (4.4)$$

where

$$\mathbf{J}_s = -\frac{1}{2i}(\psi^*\nabla\psi - \psi\nabla\psi^*) - |\psi|^2\mathbf{A} = -\Im[\psi^*(\nabla + i\mathbf{A})\psi], \quad (4.5)$$

with the corresponding gauge condition,

$$\varepsilon\sigma\phi + \nabla \cdot \mathbf{A} = 0. \quad (4.6)$$

The boundary conditions associated with Eqs. (4.3) and (4.4) are

$$\mathbf{n} \cdot (\nabla + i\mathbf{A})\psi = 0, \quad \mathbf{n} \times (\nabla \times \mathbf{A}) = \mathbf{n} \times \mathbf{H}, \quad \mathbf{n} \cdot \mathbf{A} = 0. \quad (4.7)$$

The electromagnetic variables are given by the expressions

$$\mathbf{B} = \nabla \times \mathbf{A}, \quad \mathbf{J} = \nabla \times \nabla \times \mathbf{A}, \quad \mathbf{E} = -\partial_t\mathbf{A} - \varepsilon\nabla\phi. \quad (4.8)$$

**Reduction to homogeneous form.** Next, we homogenize the problem. Let  $\mathbf{A}_0$  be the (unique) minimizer of the convex quadratic form  $Q_1 \equiv Q_1[\mathbf{A}]$ ,

$$Q_1[\mathbf{A}] = \int_{\Omega} [(\nabla \cdot \mathbf{A})^2 + |\nabla \times \mathbf{A} - \mathbf{H}|^2] \, d\mathbf{x}, \quad (4.9)$$

on  $\text{dom}(Q_1) = \{\mathbf{A} \in [W^{1,2}(\Omega)]^n : \mathbf{n} \cdot \mathbf{A} = 0 \text{ on } \partial\Omega\}$ . This minimizer satisfies the boundary-value problem

$$\nabla \times \nabla \times \mathbf{A} - \nabla \times \mathbf{H} = \mathbf{0}, \quad \nabla \cdot \mathbf{A} = 0 \quad \text{in } \Omega, \quad (4.10)$$

$$\mathbf{n} \times (\nabla \times \mathbf{A}) = \mathbf{n} \times \mathbf{H}, \quad \mathbf{n} \cdot \mathbf{A} = 0 \quad \text{on } \partial\Omega, \quad (4.11)$$

in the dual of  $\text{dom}(Q_1)$  with respect to the inner product in  $[L^2(\Omega)]^n$ . The mapping  $\mathbf{H} \mapsto \mathbf{A}_0$  is linear, time independent, and continuous from  $[W^{\alpha,2}(\Omega)]^n$  to  $[W^{1+\alpha,2}(\Omega)]^n$  [16]. The contribution of the vector  $\mathbf{A}_0$  to the magnetic field is

$$\mathbf{B}_0 = \nabla \times \mathbf{A}_0. \quad (4.12)$$

We substitute variables,

$$\mathbf{A} = \mathbf{A}_0 + \varepsilon \mathbf{A}', \quad (4.13)$$

and rewrite the (scaled) TDGL equations (4.3)–(4.7) in terms of  $\psi$  and  $\mathbf{A}'$  (omitting the primes),

$$\partial_t \psi + i\sigma^{-1}(\nabla \cdot (\varepsilon \mathbf{A}))\psi - (\nabla + i(\mathbf{A}_0 + \varepsilon \mathbf{A}))^2 \psi - (1 - |\psi|^2)\psi = 0 \quad \text{in } \Omega, \quad (4.14)$$

$$\sigma \partial_t \mathbf{A} - \Delta \mathbf{A} - \mathbf{J}_s = \mathbf{0} \quad \text{in } \Omega, \quad (4.15)$$

where

$$\mathbf{J}_s = -\frac{1}{2i}(\psi^* \nabla \psi - \psi \nabla \psi^*) - |\psi|^2(\mathbf{A}_0 + \varepsilon \mathbf{A}), \quad (4.16)$$

and

$$\mathbf{n} \cdot \nabla \psi = 0, \quad \mathbf{n} \times (\nabla \times \mathbf{A}) = \mathbf{0}, \quad \mathbf{n} \cdot \mathbf{A} = 0 \quad \text{on } \partial\Omega. \quad (4.17)$$

**Functional formulation.** We reformulate the system of Eqs. (4.14)–(4.17) as an ordinary differential equation for a vector-valued function  $u = (\psi, \mathbf{A})$  from the time domain  $(0, \infty)$  to a space of functions on  $\Omega$ ,

$$u = (\psi, \mathbf{A}) : [0, \infty) \rightarrow \mathcal{L}^2 = [L^2(\Omega)]^2 \times [L^2(\Omega)]^n. \quad (4.18)$$

The equation is

$$\frac{du}{dt} + Au = f_0(u) + \varepsilon f_1(u), \quad (4.19)$$

where  $A$  is the linear operator in  $\mathcal{L}^2$  associated with the quadratic form  $Q \equiv Q[u]$ ,

$$Q[u] = \int_{\Omega} \left[ |\nabla \psi|^2 + \sigma^{-1} \left( (\nabla \cdot \mathbf{A})^2 + |\nabla \times \mathbf{A}|^2 \right) \right] d\mathbf{x}, \quad (4.20)$$

on  $\text{dom}(Q) = \{u = (\psi, \mathbf{A}) \in \mathcal{L}^2 : \mathbf{n} \cdot \mathbf{A} = 0 \text{ on } \partial\Omega\}$ . The functions  $f_0$  and  $f_1$  are nonlinear,

$$f_i(u) = (\varphi_i(\psi, \mathbf{A}), \sigma^{-1} \mathbf{F}_i(\psi, \mathbf{A})), \quad i = 0, 1, \quad (4.21)$$

where

$$\varphi_0(\psi, \mathbf{A}) = 2i\mathbf{A}_0 \cdot (\nabla \psi) - |\mathbf{A}_0|^2 \psi + (1 - |\psi|^2) \psi, \quad (4.22)$$

$$\varphi_1(\psi, \mathbf{A}) = i(1 - \sigma^{-1})(\nabla \cdot \mathbf{A})\psi + 2i\mathbf{A} \cdot (\nabla \psi) - (\mathbf{A}_0 \cdot \mathbf{A})\psi - |\mathbf{A}|^2 \psi, \quad (4.23)$$

$$\mathbf{F}_0(\psi, \mathbf{A}) = 0, \quad (4.24)$$

$$\mathbf{F}_1(\psi, \mathbf{A}) = -\frac{1}{2i}(\psi^* \nabla \psi - \psi \nabla \psi^*) - |\psi|^2(\mathbf{A}_0 + \varepsilon \mathbf{A}). \quad (4.25)$$

Given any  $f = (\varphi, \sigma^{-1} \mathbf{F}) \in \mathcal{L}^2$ , the equation  $Au = f$  is equivalent with the system of uncoupled boundary-value problems

$$-\Delta \psi = \varphi \text{ in } \Omega, \quad \mathbf{n} \cdot \nabla \psi = 0 \text{ on } \partial\Omega, \quad (4.26)$$

$$-\Delta \mathbf{A} = \mathbf{F} \text{ in } \Omega, \quad \mathbf{n} \times \mathbf{A} = \mathbf{0}, \quad \mathbf{n} \cdot \mathbf{A} = 0 \text{ on } \partial\Omega, \quad (4.27)$$

in the dual of  $\text{dom}(Q)$  with respect to the inner product in  $\mathcal{L}^2$ . The operator  $A$  is selfadjoint and positive definite in  $\mathcal{L}^2$ ; hence, its fractional powers  $A^{\theta/2}$  are well defined, they are unbounded if  $\theta \geq 0$ , and  $\text{dom}(A^{\theta/2})$  is a closed linear subspace of  $\mathcal{W}^{\theta,2} = [W^{\theta,2}(\Omega)]^2 \times [W^{\theta,2}(\Omega)]^n$ ; see [17, Section 1.4].

The solution of Eq. (4.19) depends on  $\varepsilon$ ; we denote it by  $u_\varepsilon$ . We compare  $u_\varepsilon$  with the solution  $u_0$  of the reduced equation

$$\frac{du}{dt} + Au = f_0(u). \quad (4.28)$$

**Theorem 4.1** *There exists a positive constant  $C$  such that*

$$\|u_\varepsilon(t) - u_0(t)\|_{\mathcal{W}^{1+\alpha,2}} \leq C (\|u_\varepsilon(0) - u_0(0)\|_{\mathcal{W}^{1+\alpha,2}} + \varepsilon), \quad t \in [0, T]. \quad (4.29)$$

**Proof.** Let  $B_R$  be the ball of radius  $R$  centered at the origin in  $\mathcal{W}^{1+\alpha,2}$ . Let  $u_\varepsilon \in B_R$  and  $u_0 \in B_R$  satisfy Eqs. (4.19) and (4.28), respectively, with initial data  $u_\varepsilon(0)$  and  $u_0(0)$ . The difference  $v = u_\varepsilon - u_0$  satisfies the differential equation

$$\frac{dv}{dt} + Av = f_0(u_\varepsilon) - f_0(u_0) + \varepsilon f_1(u_\varepsilon) \quad (4.30)$$

or, equivalently, the integral equation

$$v(t) = e^{-tA}v(0) + \int_0^t e^{-(t-s)A}[f_0(u_\varepsilon) - f_0(u_0) + \varepsilon f_1(u_\varepsilon)](s) \, ds. \quad (4.31)$$

From the integral equation we obtain the estimate

$$\begin{aligned} \|v(t)\|_{\mathcal{W}^{1+\alpha,2}} &\leq \|e^{-tA}\|_{\mathcal{W}^{1+\alpha,2}} \|v(0)\|_{\mathcal{W}^{1+\alpha,2}} + \int_0^t \|A^{(1+\alpha)/2} e^{-(t-s)A}\|_{\mathcal{W}^{1+\alpha,2}} \\ &\quad \times [\|f_0(u_\varepsilon) - f_0(u_0)\|_{L^2} + \varepsilon \|f_1(u_\varepsilon)\|_{L^2}] (s) \, ds. \end{aligned} \quad (4.32)$$

The operator norms satisfy the inequalities

$$\|e^{-tA}\|_{\mathcal{W}^{1+\alpha,2}} \leq 1, \quad \|A^{(1+\alpha)/2} e^{-(t-s)A}\|_{\mathcal{W}^{1+\alpha,2}} \leq C(t-s)^{-(1+\alpha)/2}; \quad (4.33)$$

see [17, Theorem 1.4.3]. Furthermore, adding and subtracting terms, we have

$$\begin{aligned} f_0(u_\varepsilon) - f_0(u_0) &= \left( 2i\mathbf{A}_0 \cdot (\nabla(\psi_\varepsilon - \psi_0)) - |\mathbf{A}_0|^2(\psi_\varepsilon - \psi_0) \right. \\ &\quad \left. + (1 - |\psi_\varepsilon|^2 - |\psi_0|^2)(\psi_\varepsilon - \psi_0) - \psi_\varepsilon \psi_0(\psi_\varepsilon^* - \psi_0^*), 0 \right), \end{aligned} \quad (4.34)$$

where

$$\begin{aligned} \|2i\mathbf{A}_0 \cdot (\nabla(\psi_\varepsilon - \psi_0))\|_{L^2} &\leq 2\|\mathbf{A}_0\|_{L^\infty} \|\psi_\varepsilon - \psi_0\|_{W^{1,2}} \\ &\leq C\|\psi_\varepsilon - \psi_0\|_{W^{1+\alpha,2}} \leq C\|u_\varepsilon - u_0\|_{\mathcal{W}^{1+\alpha,2}}, \\ \| |\mathbf{A}_0|^2(\psi_\varepsilon - \psi_0) \|_{L^2} &\leq C\|\mathbf{A}_0\|_{L^\infty}^2 \|\psi_\varepsilon - \psi_0\|_{L^\infty} \\ &\leq C\|\psi_\varepsilon - \psi_0\|_{W^{1+\alpha,2}} \leq C\|u_\varepsilon - u_0\|_{\mathcal{W}^{1+\alpha,2}}, \end{aligned}$$

and the other terms are estimated similarly. Here,  $C$  is some (generic) positive constant, which may depend on  $\mathbf{H}$  and  $\Omega$  but not on  $u_\varepsilon$  or  $u_0$ . (In these inequalities we have used the continuity of the imbedding of  $W^{1+\alpha,2}$  into  $W^{1,2} \cap L^\infty$ .) The result is an inequality of the type

$$\|f_0(u_\varepsilon) - f_0(u_0)\|_{L^2} \leq C\|u_\varepsilon - u_0\|_{\mathcal{W}^{1+\alpha,2}}, \quad (4.35)$$

showing that  $f_0$  is Lipschitz from  $\mathcal{W}^{1+\alpha,2}$  to  $\mathcal{L}^2$ .

Using similar estimates, we show that  $f_1$  is bounded from  $\mathcal{W}^{1+\alpha,2}$  to  $\mathcal{L}^2$ , so there exists a positive constant  $C$  such that

$$\|f_1(u_\varepsilon)\|_{L^2} \leq C. \quad (4.36)$$

Combining the estimates (4.33), (4.35), and (4.36) with the inequality (4.32), we conclude that there exist positive constants  $C_1$  and  $C_2$  such that

$$\|v(t)\|_{\mathcal{W}^{1+\alpha,2}} \leq \|v(0)\|_{\mathcal{W}^{1+\alpha,2}} + \varepsilon C_1 t^{(1-\alpha)/2} + C_2 \int_0^t (t-s)^{-(1+\alpha)/2} \|v(s)\|_{\mathcal{W}^{1+\alpha,2}} \, ds. \quad (4.37)$$

Applying Gronwall's inequality, we obtain the estimate

$$\|v(t)\|_{\mathcal{W}^{1+\alpha,2}} \leq C (\|v(0)\|_{\mathcal{W}^{1+\alpha,2}} + \varepsilon), \quad t \in [0, T], \quad (4.38)$$

for some positive constant  $C$ . ■

It follows from Theorem 4.1 that, if the initial data are such that  $\|u_\varepsilon(0) - u_0(0)\|_{\mathcal{W}^{1+\alpha,2}} = o(1)$  as  $\varepsilon \downarrow 0$ , then

$$\lim_{\varepsilon \rightarrow 0} u_\varepsilon = u_0 \quad (4.39)$$

in  $C([0, T]; \mathcal{W}^{1+\alpha,2})$  for any  $T > 0$ . In particular, if  $\|u_\varepsilon(0) - u_0(0)\|_{\mathcal{W}^{1+\alpha,2}} = O(\varepsilon)$ , then the convergence in Eq. (4.39) is  $O(\varepsilon)$ .

## 4.2 Interpretation and final remarks

It remains to translate the results back in terms of the original variables. We denote the solution of the TDGL equations, Eqs. (2.13)–(2.18), by  $\psi_\kappa$ ,  $\mathbf{A}_\kappa$ ,  $\phi_\kappa$ . The variables  $\mathbf{A}_\kappa$  and  $\phi_\kappa$  are related by the gauge condition  $\sigma\phi_\kappa + \nabla \cdot \mathbf{A}_\kappa = 0$  at all times. Let  $\mathbf{B}_\kappa = \nabla \times \mathbf{A}_\kappa$ .

Let  $\mathbf{A}_\infty$  be the solution of the boundary-value problem

$$\nabla \times \nabla \times \mathbf{A} - \nabla \times \mathbf{H} = \mathbf{0}, \quad \nabla \cdot \mathbf{A} = 0 \quad \text{in } \Omega, \quad (4.40)$$

$$\mathbf{n} \times (\nabla \times \mathbf{A}) = \mathbf{n} \times \mathbf{H}, \quad \mathbf{n} \cdot \mathbf{A} = 0 \quad \text{on } \partial\Omega, \quad (4.41)$$

and put  $\mathbf{B}_\infty = \nabla \times \mathbf{A}_\infty$ . The vector  $\mathbf{A}_\infty$  and, hence,  $\mathbf{B}_\infty$  do not vary with time. Let  $\psi_\infty$  satisfy the equations

$$\partial_t \psi - \Delta_{\mathbf{A}_\infty} \psi - (1 - |\psi|^2)\psi = 0 \quad \text{in } \Omega, \quad \mathbf{n} \cdot \nabla_{\mathbf{A}_0} \psi = 0 \quad \text{on } \partial\Omega. \quad (4.42)$$

Then it follows from Theorem 4.1 that there exists a positive constant  $C$  such that

$$\|\psi_\kappa(t) - \psi_\infty(t)\|_{W^{1+\alpha,2}} + \frac{\|\mathbf{B}_\kappa(t) - \mathbf{B}_\infty\|_{W^{\alpha,2}}}{\|\mathbf{H}\|_{W^{\alpha,2}}} \quad (4.43)$$

$$\leq C \left( \|\psi_\kappa(0) - \psi_\infty(0)\|_{W^{1+\alpha,2}} + \frac{\|\mathbf{B}_\kappa(0) - \mathbf{B}_\infty\|_{W^{\alpha,2}}}{\|\mathbf{H}\|_{W^{\alpha,2}}} + \frac{1}{\kappa^2} \right), \quad (4.44)$$

for all  $t \in [0, T]$ ,  $T > 0$ .

The approximation  $(\psi_\infty, \mathbf{B}_\infty)$  is the “frozen-field approximation.” Hence, the analysis shows that the solution of the TDGL equations converges to the frozen-field approximation, uniformly on compact time intervals  $[0, T]$  in the topology of  $[W^{1+\alpha,2}(\Omega)]^2 \times [W^{\alpha,2}(\Omega)]^n$ , as soon as the initial data satisfy the asymptotic estimates  $\|\psi_\kappa(0) - \psi_\infty(0)\|_{W^{1+\alpha,2}} = o(1)$  and  $\|\mathbf{B}_\kappa(0) - \mathbf{B}_\infty\|_{W^{\alpha,2}} = o(\kappa)$  as  $\kappa \rightarrow \infty$ . Under slightly sharper conditions we obtain the order of convergence.

**Corollary 4.1** *If*

$$\|\psi_\kappa(0) - \psi_\infty(0)\|_{W^{1+\alpha,2}} = O\left(\frac{1}{\kappa^2}\right) \quad \text{and} \quad \frac{\|\mathbf{B}_\kappa(0) - \mathbf{B}_\infty\|_{W^{\alpha,2}}}{\|\mathbf{H}\|_{W^{\alpha,2}}} = O\left(\frac{1}{\kappa^2}\right)$$

*as  $\kappa \rightarrow \infty$ , then*

$$\|\psi_\kappa(t) - \psi_\infty(t)\|_{W^{1+\alpha,2}} + \frac{\|\mathbf{B}_\kappa(t) - \mathbf{B}_\infty\|_{W^{\alpha,2}}}{\|\mathbf{H}\|_{W^{\alpha,2}}} = O\left(\frac{1}{\kappa^2}\right), \quad (4.45)$$

*uniformly on compact intervals.*

This result explains the numerical results presented in Section 3.

**Remark 1.** The asymptotic approximation procedure can be continued to higher order, as can be seen from a formal expansion. The equations for the order parameter and the vector potential decouple, and at each order one finds first the vector potential, then the order parameter. The vector potential satisfies a linear heat equation; for example, the first correction beyond  $\mathbf{A}_\infty$  is  $\kappa^{-1}\mathbf{A}$ , where  $\mathbf{A}$  satisfies the equation

$$-\sigma\partial_t\mathbf{A} + \Delta\mathbf{A} = \Im[\psi_\infty^* \nabla_{\mathbf{A}_\infty} \psi_\infty]. \quad (4.46)$$

**Remark 2.** The analysis given here differs at several points from the analysis of Ref. [10]. First, our scaling is slightly different and, we believe, more in tune with the physics; second, our regularity assumptions on the applied field are weaker; third, our proofs are more direct; and fourth, our results hold in a stronger topology.

## Acknowledgments

We thank Professor Todd Dupont (University of Chicago) for stimulating discussions throughout the course of this investigation. We also acknowledge the work of Damien

Declat (student from ISTIL, Lyon, France), who assisted in the development of an earlier version of the parallel computer program.

This work was supported by the Mathematical, Information, and Computational Sciences Division subprogram of the Office of Advanced Scientific Computing Research, U.S. Department of Energy, under Contract W-31-109-Eng-38. The second author was partially supported by the University of Chicago/Argonne National Laboratory Collaborative Grant No. 96-011.

## References

- [1] D.W. Braun, G.W. Crabtree, H.G. Kaper, A.E. Koshelev, G.K. Leaf, D.M. Levine and V.M. Vinokur, Structure of a moving vortex lattice. *Phys. Rev. Lett.* 76 (1996) 831–834.
- [2] G.W. Crabtree, D.O. Gunter, H.G. Kaper, A.E. Koshelev, G.K. Leaf and V.M. Vinokur, Numerical solution of driven vortex systems. *Phys. Rev. B* 61 (2000) 1446–1455.
- [3] I. Aranson and V. Vinokur, Surface instabilities and plastic deformation of vortex lattices. *Phys. Rev. Lett.* 77 (1996) 3208–3211.
- [4] M. Tinkham, *Introduction to Superconductivity* (2nd ed.). New York: McGraw-Hill (1996) xxi+454pp.
- [5] V.L. Ginzburg and L.D. Landau, On the theory of superconductivity. *Zh. Eksp. Teor. Fiz.* (USSR) 20 (1950) 1064–1082; Engl. transl. in: D. ter Haar, *L. D. Landau; Men of Physics* (Vol. I). Oxford: Pergamon Press (1965) pp. 138–167.
- [6] Q. Du, M.D. Gunzburger and J.S. Peterson, Analysis and approximation of the Ginzburg–Landau model of superconductivity. *SIAM Review* 34 (1992) 54–81.
- [7] Q. Du, Global existence and uniqueness of solutions of the time-dependent Ginzburg–Landau model for superconductivity. *Appl. Anal.* 53 (1994) 1–18.
- [8] Q. Tang and S. Wang, Time-dependent Ginzburg–Landau equations of superconductivity. *Physica D* 88 (1995) 139–166.
- [9] J. Fleckinger–Pellé, H.G. Kaper and P. Takáč, Dynamics of the Ginzburg–Landau equations of superconductivity. *Nonlinear Analysis: Theory, Methods & Applications* 32 (1998) 647–665.



- [10] Q. Du and P. Gray, High-kappa limits of the time-dependent Ginzburg–Landau model. *SIAM J. of Appl. Math.* 56 (1996) 1060–1093.
- [11] A. Schmid, A time dependent Ginzburg–Landau equation and its application to a problem of resistivity in the mixed state. *Phys. kondens. Materie* 5 (1966) 302–317.
- [12] L.P. Gor’kov and G.M. Eliashberg, Generalizations of the Ginzburg–Landau equations for non-stationary problems in the case of alloys with paramagnetic impurities. *Zh. Eksp. Teor. Fiz.* 54 612–626 (1968); *Soviet Phys.—JETP* 27 (1968) 328–334.
- [13] L.P. Gor’kov and N. Kopnin, Vortex motion and resistivity of type-II superconductors in a magnetic field. *Soviet Phys.—Usp.* 18 (1976) 496–513.
- [14] V.L. Ginzburg, On the destruction and the onset of superconductivity in a magnetic field. *Soviet Phys.—JETP* 34(7) (1958) 78–87.
- [15] S.J. Chapman, Superheating field of type-II superconductors. *SIAM J. of Appl. Math.* 55 (1995) 1233–1258.
- [16] V. Georgescu, Some boundary value problems for differential forms on compact Riemannian manifolds. *Ann. Mat. Pura Appl.* 122(4) (1979) 159–198.
- [17] D. Henry, *Geometric Theory of Semilinear Parabolic Equations*. Lecture Notes in Mathematics, Vol. 840. New York: Springer-Verlag (1981) 348pp.